

UDC 535.2:616-71

INFORMATION SYSTEM FOR MULTI-VECTOR RAYTRACING IN ELLIPSOIDAL REFLECTORS¹⁾Poluektov S.O., ¹⁾Bezugla N.V., ²⁾Kurowska-Wilczyńska K. and ¹⁾Bezuglyi M.O.¹⁾ National Technical University of Ukraine "Igor Sikorsky Kyiv Polytechnic Institute",
Kyiv, Ukraine²⁾ SWPS University, Warsaw, PolandE-mail: m.bezuglyi@kpi.ua

Due to two focuses, ellipsoidal reflectors are unique reflective optical elements that allow conjugate imaging in two focal planes within their inner cavity. Such reflectors are used in various devices, such as lens telescopes, to achieve high resolution. They have found applications in microscope optical systems to increase the depth of field. They are used in scientific instruments, such as laser systems, to ensure the laser beam's high accuracy and stability. Despite their advantages, the non-spherical shape of ellipsoidal reflectors also introduces drawbacks in the form of errors arising from raytracing on the side surface. It complicates aberration analysis and necessitates specialized software for multi-vector ray tracing. Considering the deviations in the coordinates of the intersections between rays and the second focal plane allows for optimizing the reflector design to achieve maximum efficiency. Therefore, this work aims to enhance the efficiency of the aberration analysis of ellipsoidal reflectors by developing principles and informational tools for multi-vector ray tracing.

The article presents the results of developing an information system for multi-vector analysis in ellipsoidal reflectors. The developed multi-vector algorithm enables selecting tracing modes, tuning launch parameters, and setting the step size for launching rays. The specialized software features for single- and multi-vector raytracing in an ellipsoidal reflector are presented. The side surface of the ellipsoid is the object under study. The software provides the capability to realize different methods of multi-vector ray tracing, such as radius-based, diameter-based, and partial radius-based, for different types of tasks, thereby expanding the possibilities for visualizing the simulation results.

Based on the multi-vector aberration analysis of the side surface of the ellipsoidal reflector, the center coordinates and root mean square deviations were obtained for different reflection acts when changing the zenith angle of tracing. The influence of zenith angles on coordinate variations was assessed, which can be realized in selecting parameters for ellipsoidal reflectors and designing the optical system of photometers for various purposes. It can also aid in developing additional means to compensate for aberrations or modify the reflector's side surface shape.

Keywords: ellipsoidal reflector; raytracing; multi-vector; aberration analysis; Centroid; RMS.

Introduction

Non-spherical optical systems achieve high image quality that cannot be achieved with traditional spherical systems [1, 2]. These systems consist of geometrically complex surfaces, and their design involves various technical and technological challenges related to manufacturing, shape control, aberration compensation, etc. [2 - 5]. Optical elements of non-spherical shapes have found wide applications in mirrors and reflectors, which have aspheric forms, meaning their surfaces represent complex mathematical curves that cannot be obtained by simply changing the radius of a spherical surface [6, 7]. Non-spherical reflectors can have different forms, depending on the variation of the conic constant k according to the surface profile equation, such as parabolic ($k = -1$), hyperbolic ($k < -1$), or elliptical ($k > 0$).

An essential element of non-spherical optics is the ellipsoidal reflector (ER), with an internal reflecting surface characterized by two focuses the presence that forms two focal planes perpendicular to the ellipsoid major axis [7]. The focuses are located on

the ellipsoid major axis and have the same focal distance f from the ER center, allowing an object placed in one focal plane to have an image formed in the other. This property gives ER an advantage over different types of reflectors and finds wide application in the design of biomedical photometers, telescopes, and various optical systems where achieving high image quality and efficient concentration of light flux is essential [7 - 10]. Like other optical elements, ER is subject to various types of aberrations, such as spherical aberration, coma, and astigmatism, which degrade the image quality and require the development of specialized compensation algorithms. These algorithms can be developed based on the raytracing properties study of the ER surface [11 - 14].

In photonics and optical engineering software, raytracing simulates electromagnetic (optical) wavefronts propagation through a system [12]. Rays are represented as lines constructed using discrete points on surfaces, representing the wavefront's local position as it propagates through the optical system [15 -19].

Raytracing is an effective method for investigating reflectors, as it allows for modeling the light propagation in complex optical systems, including ellipsoidal reflectors [20]. During raytracing in ER, the path of a ray that emerges from the first focal plane reflects off the reflector side surface and intersects the second focal plane at a certain point is determined [17, 19]. The coordinates of this point serve as the basis for calculating the deviation of its position from the coordinates in an ideal system, which is a characteristic of aberrations.

Aberration analysis of the ellipsoidal reflectors' side surface through the investigation of raytracing properties will allow for the improvement of ER designs and optical systems of various photometers by designing additional means for aberration compensation or modifying the reflector's side surface shape [8, 20].

Based on the above, this article aims to enhance the ellipsoidal reflectors' aberration analysis efficiency by developing principles and informational systems for multi-vector raytracing on their side surface.

Multi-vector ray tracing algorithm in ellipsoidal reflector

A wide range of data is required to multi-vector aberration analysis of the ER side surface, which involves significant time investment. Therefore, a multi-vector raytracing algorithm in an ellipsoidal reflector has been developed in this work. A cavity ellipsoid of revolution forms the reflector shape with an internal mirror surface and orthogonal planes at focal distances from the ellipsoid center. In other words, the focal planes are located at the perifocal distance from the intersection points of the major ellipsoid axis with the side surface [11 - 14].

Figure 1 illustrates the algorithm for multi-vector raytracing in ellipsoidal reflectors, which begins with the ellipsoid geometric parameters' adjustment, particularly the major a , and the minor b axis, followed by the focal distance f , focal parameter p , and eccentricity e calculation.

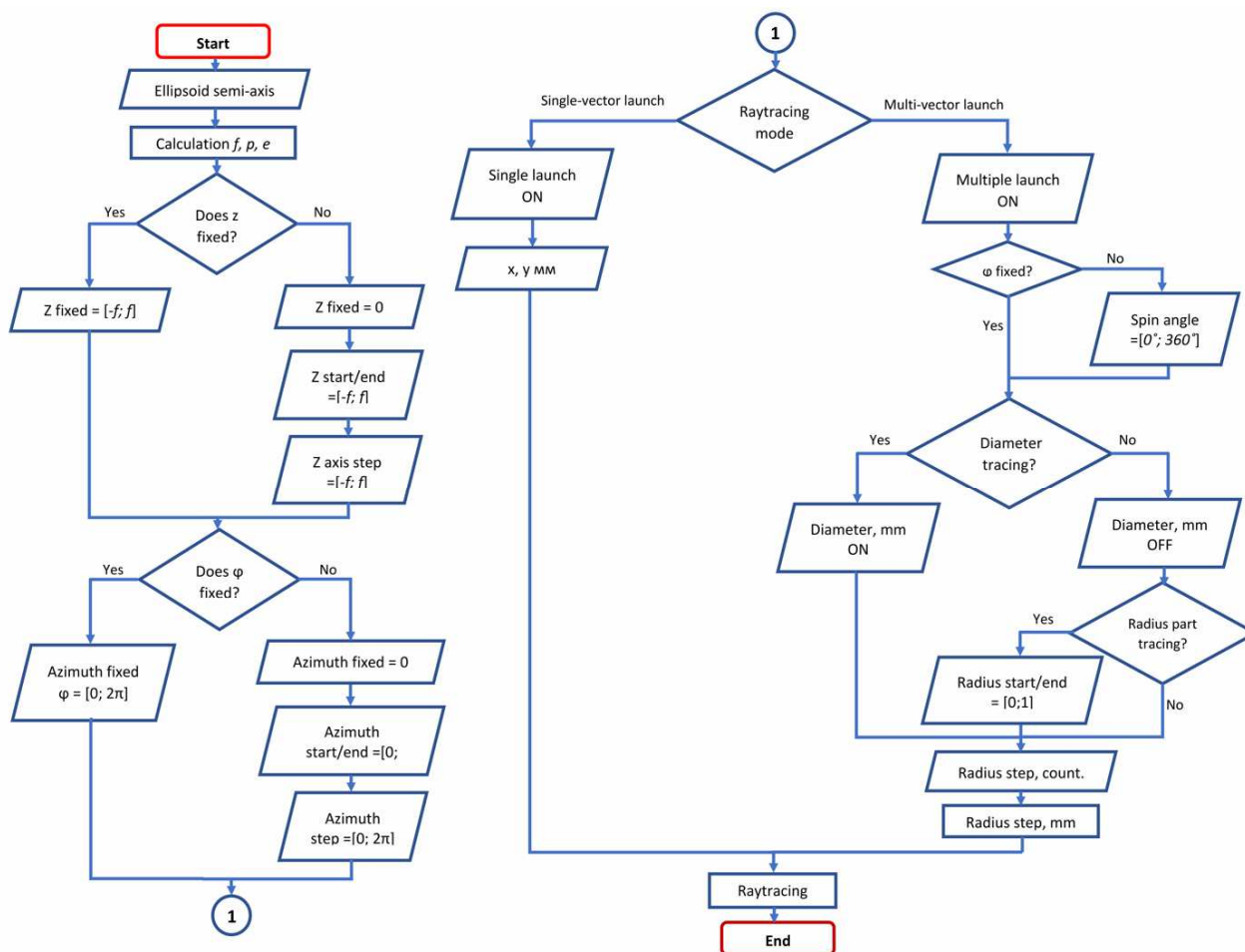


Fig. 1. Multi-vector raytracing algorithm in ellipsoidal reflector

The next step is to determine the need for fixing the Z-axis. Suppose it is necessary to compute the

intersection of rays with a specific plane at a certain distance from the ellipsoid center. In that case, the

value is entered in the "z fixed, mm" field, which belongs to the interval $[-f, f]$, where f – focal parameter. Otherwise, we check that "z fixed, mm" is set to 0 and enter the step size of the ap-axis, which determines the spacing between the ray intersection planes for determining the zenith angles θ of the tracing, in the "z axis step, mm" field. If it is necessary to examine the ellipsoid side surface part, the initial "z start, mm" and final "z end, mm" values of the interval are entered (by default, $z \in [-f, f]$).

The next step is determining the need to fix the azimuthal angle φ . When setting the azimuthal angle, the rays are launched from points on the radius without rotation within the full azimuthal angle range. To fix it, the "Azimuth fixed φ , rad $\cdot\pi$ " is entered, which represents the angle by which we rotate the initial ray launch point - in the case of a single-vector launch, or the inclination angle of the radius vector of the initial points - in the case of a multi-vector launch. Suppose there is no need to fix the azimuthal angle φ . In that case, it is checked whether "Azimuth fixed φ , rad $\cdot\pi$ " is set to 0, and the initial "Azimuth start φ , rad $\cdot\pi$ " and final "Azimuth end φ , rad $\cdot\pi$ " rotation angles of the initial points are entered. Additionally, the step size for the rotation is specified in the "Azimuth step, rad $\cdot\pi$ " field, with values ranging from 0 to 2π ($\varphi \in [0; 2\pi]$).

Next, the method for raytracing in the ellipsoidal reflector is selected. A "Single launch" means the raytracing will be performed from a single initial point. To set this mode, press "Single launch" and enter the initial coordinates in the "x, mm" and "y, mm" fields. Multiple launch means that the launch occurs from an array of initial points along the radius vector. To select this mode, press "Multiple launch." The next step is to check if the azimuthal angle is fixed (the angle between the radius vector and the x-axis for the mode without rotating the initial points within the full azimuthal angle range). If "Azimuth fixed φ , rad $\cdot\pi$ " is set to 0, enter the inclination angle of the radius vector in the "Spin angle, deg" field, ranging from 0° to 360° .

There is also an option to raytracing from points lying on the diameter by activating "Diameter, mm." Additionally, a specific range along the radius vector can choose where the initial points will be selected. To do this, enter the start "Radius start" and end "Radius end" values of the interval. The values range from 0 to 1, where 1 represents the total length of the radius vector. Specify the step size for selecting points on the radius vector/diameter by entering the desired number of points in the "Radius step, count" field. After entering the value in the "Radius step, mm" field, the step size in millimeters will be automatically calculated. In the case of launching from the diameter, the number of steps will be automatically doubled. Once the parameter setup is complete, click the "GO" button to start the computation. It marks the

completion of the parameter configuration stage and initiates the calculation process.

Software RTER v.2.0

Based on the developed algorithm (Figure 1), the "RayTracing in Ellipsoidal Reflector" (RTER v.2.0) software has been produced for single and multiple vector raytracing in an ellipsoidal reflector [21]. The ellipsoid side surface serves as the goal object for research. The input data include the ellipsoid geometric parameters and the configuration of the initial launch points (steps, angles, and intervals). The output data consists of the weight center position of the scattering spot in the focal plane (Centroid), each point's root mean square (RMS) deviation, and the count of reflection events that occurred during raytracing. The software also allows for saving the count of rays that underwent a certain reflection acts number at each step along the major ellipsoid axis and provides the ability to analyze these data for each step along the radius vector. Additionally, the software delivers results for calculating the RMS and Centroid indicators based on the reflection acts number for each step along the radius vector.

The tab panel (Figure 2) is a functional interface element that allows users to view and switch between tabs, make necessary changes to the program's functionality, and input relevant data for calculations. It consists of 6 tabs: "General" – a tab for entering and calculating the ellipsoid parameters, selecting the tracing mode, and entering the necessary data for calculations; "Graph parameters" – a tab for configuring the axes, circles, and graph scale; "Result" – a tab for selecting the desired calculation results and specifying file paths for saving; "Colorized" – a tab for setting the points color on the graph corresponding to different numbers of reflection acts and displaying their total count; "RMS" – a tab for calculation results outputting of the ellipsoid's RMS and the total count of reflection acts; "Centroid" – a tab for calculation results outputting of the ellipsoid's centroid and the total count of reflection acts.

When the start button is activated, the modeling process begins, and the calculation duration depends on the chosen accuracy. After the modeling, an image representing the intersection of rays with the plane along the major ellipsoid axis and the second focal plane will be displayed in the window (3).

The "General" tab (Figure 3) is designed to input and calculate the ellipsoid parameters, select the tracing mode, and enter the relevant data for calculations.

The "Ellipsoid semi-axis" fields (1), especially "Semi-major axis a , mm" and "Semi-minor axis b , mm," are input fields for entering the major a and minor b ellipsoid axis values in millimeters. The ellipsoid parameters are automatically calculated after entering the data in the "Ellipsoid parameters" fields (2).

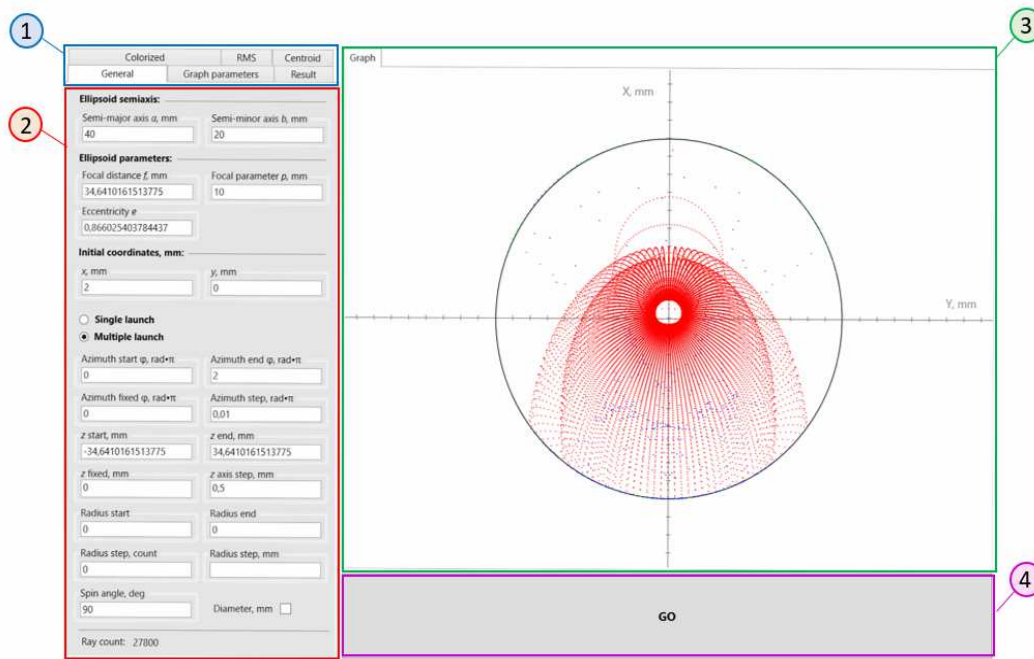


Fig. 2. RTER v.2.0 software main window: 1 – tabs panel; 2 – tab content; 3 – graphic result display window; 4 – button to the calculation start.

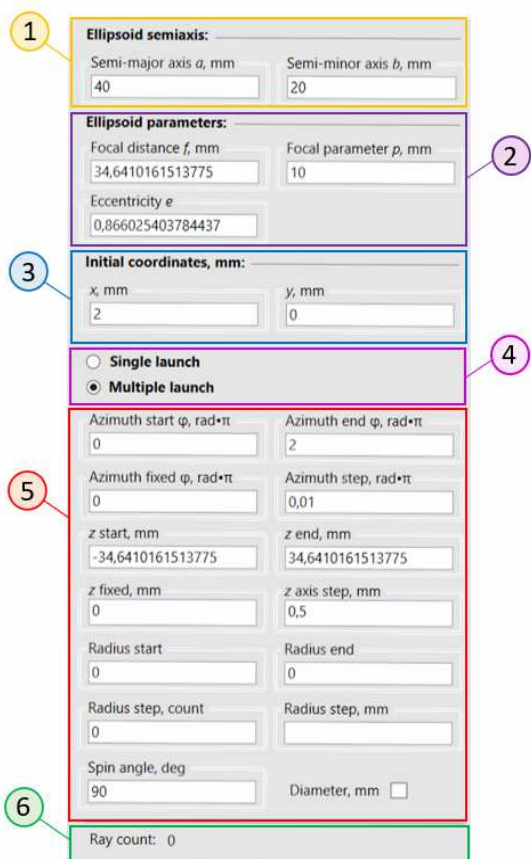


Fig. 3. "General" tab input fields: 1 – "Ellipsoid semi-axis" fields; 2 – "Ellipsoid parameters" fields; 3 – "Initial coordinates, mm" fields; 4 – tracing mode selection fields; 5 – launch parameter input fields; 6 – "Ray count" fields

These parameters include "Focal distance f , mm," which is the distance from the focus F to the ellipsoid center $O(0;0;0)$; "Focal parameter p , mm," which characterizes the radius of the ellipsoid focal circle; and "Eccentricity e " which represents the ellipsoid eccentricity. Its value can range from 0 to 1, where 0 corresponds to a circle, and 1 corresponds to a line segment. The "Initial coordinates, mm" section (3) contains input fields for the initial launch coordinates of rays from the ellipsoid first focal plane, namely "x, mm" and "y, mm."

In the tracing mode selection field (4), you can choose between "Single launch" mode, where rays are launched from a single initial point in the (3) field, or "Multiple launch" mode, where rays are launched from an array of initial points.

The launch parameter input fields (5) include cells for "Azimuth start φ , rad $\cdot\pi$ " and "Azimuth end φ , rad $\cdot\pi$." These fields enter the azimuthal angle interval relative to the x-axis in rad $\cdot\pi$ for launching rays from the ellipsoid first focal plane. The "Azimuth fixed φ , rad $\cdot\pi$ " field is used to fix the rotation angle of the initial launch point in the "Single launch" mode and to select the inclination angle of the radius vector relative to the X-axis in the "Multiple launch" mode after entering the values of "Radius step, count." The "Azimuth step, rad $\cdot\pi$ " field allows choosing the step size for the azimuthal angle of the initial launch points within the range from "Azimuth start φ , rad $\cdot\pi$ " to "Azimuth end φ , rad $\cdot\pi$." The values should range from 0 to 2π ($\varphi \in [0;2\pi]$). The fields "z start, mm" and "z end, mm" are intended for entering the range of rays intersection points with the plane at heights from $-f$ to f , with a step size of "z axis step, mm." The

"z fixed, mm" field is used to fix the rays' intersection points with a plane perpendicular to the axis of the z-axis (the major ellipsoid axis).

The "Radius start" and "Radius end" fields are used to input the interval of the radius vector. The values should range from 0 to 1, where 1 represents the radius vector's total length. The "Radius step, count" and "Radius step, mm" fields allow you to enter the number of launch points at the same distance along the radius vector within the range defined by the "Azimuth fixed φ , rad $\cdot\pi$ " angle to the x-axis. After entering the "Radius step, count," the step size in millimeters is automatically calculated and displayed in the "Radius step, mm" field. The "Spin angle, deg" represents the angle of the radius vector to the x-axis for rotating the initial launch points that belong to the radius vector within the range from "Azimuth start φ , rad $\cdot\pi$ " to "Azimuth end φ , rad $\cdot\pi$ " if "Azimuth fixed φ , rad $\cdot\pi$ " equals 0. The value is entered in degrees and should range from 0° to 360° . The "Diameter, mm" indicates the mode of launching rays from points along the diameter, which extends from the opposite quarter of the radius vector.

The "Ray count" field (6) displays the number of computed rays. The value is updated after the simulation is completed.

Raytracing methods of in ellipsoidal reflectors

The ability to use different methods of multi-raytracing in ellipsoidal reflectors is an essential feature of the software, as it affects the flexibility and adaptability of its usage [6]. Other plans allow adjusting the tracing parameters according to specific requirements and research conditions. It also expands the possibilities for visualizing the simulation results, mainly depicting intersection points between rays and the second focal plane [20]. By employing various tracing methods, precise coordinates of these points can be obtained, enabling the examination of their geometry and spatial arrangement. It is crucial for visualization and aberration analysis of the ellipsoidal reflector side surface [11-12].

Figure 4,a depicts a schematic representation of single-ray tracing, where each ray along the major ellipsoid axis has the same zenith angle. It is achieved by positioning the ray launch points at an equal distance from the center of the focal plane. In the diagram, $A(x, y)$ represents the initial launch point, rotation within the total azimuth angle with a step of φ step, and a focal parameter of p .

Single-ray launching narrows down the investigation area of the ellipsoidal reflector side surface, which may result in low representativeness.

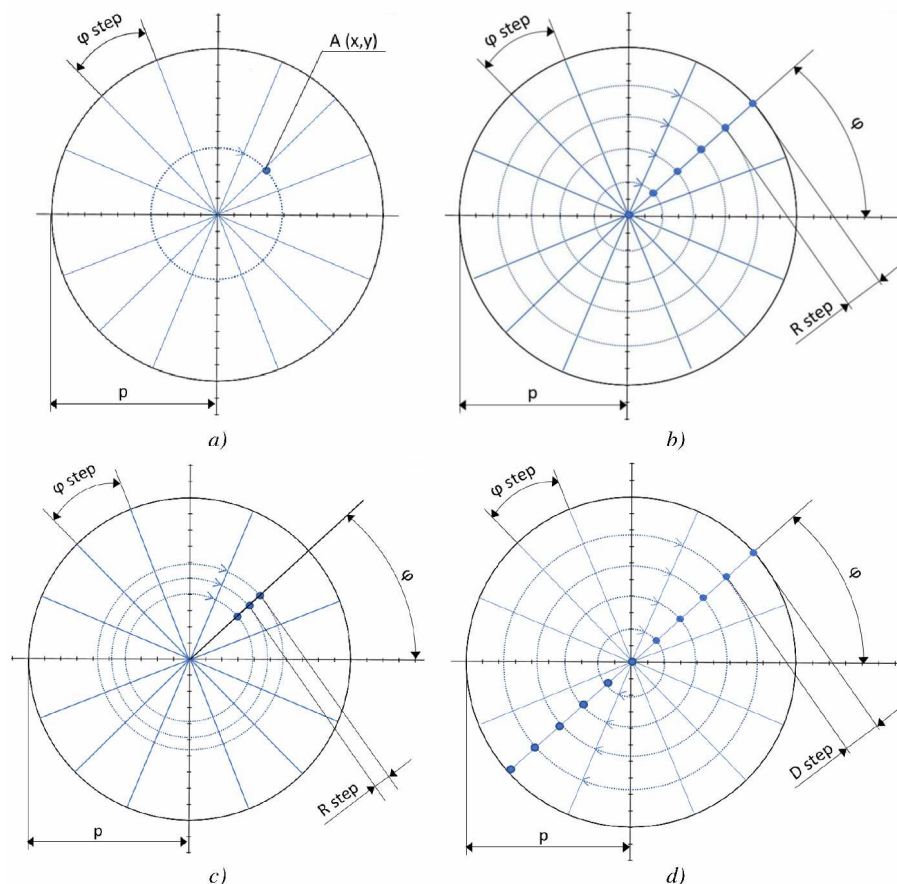


Fig. 4. Raytracing methods in ellipsoidal reflectors: single-ray (a) and multi-ray (b, c, d) tracing along the radius (b), along a radius part (c), and along the diameter (d)

The obtained results may be limited to the properties studied within that specific zone, posing challenges in generalizing the findings to a broader area. Solely relying on single-raytracing in the ER can lead to these limitations. Reducing the ER side surface can also decrease the data amount that needs to be collected and processed, thereby reducing the equipment requirements for the modeling process.

Considering the advantages and disadvantages mentioned above, the RTER v.2.0 software offers the option of using multi-raytracing to expand the functionality and automate the aberration analysis of the ellipsoidal reflector internal side surface.

Figure 4,b illustrates the schematic of multi-raytracing along the radius, where rays are launched from points at different distances from the origin by adjusting the initial points' step size (R step) on the radius vector. Thus, we have a different zenith angle θ for raytracing at each step. In the diagram, the radius vector lies at an azimuth angle φ , with rotation within the total azimuth angle at a step size of φ step, and a scalar value of p corresponding to ER focal parameter.

A specific multi-raytracing method involves launching rays from one part of the radius vector (Figure 4,c). The advantage of this method is the ability to create an intermediate stage of narrowing down the investigation zone of the ER side surface, which expands the possibilities for visualization and analysis. An advanced approach is launching rays from points belonging to the diameter (Figure 4,d). The main advantage of this method is enhanced visualization, allowing for a graphical comparison of the results obtained from launching rays along the radius vector in the Cartesian coordinate system opposite quadrants.

Ellipsoidal reflector side surface racing properties: result and discussion

Researching the tracing properties of the side surface ER is essential for understanding the rays' interaction with these surfaces. The RMS and Centroid characterize the geometric surface properties [23-25]. Investigating the tracing properties of ellipsoidal reflectors using these parameters allows for determining the optimal tracing values for maximum reflector efficiency [20]. The objective is to calculate the aberrations indicators of quantitative and statistical evaluation that arise from the reflection of the ellipsoid internal surface and are attributed to the inability of any optical system to focus broad ray beams incident at large angles into a point [12].

The zenith angle θ in optics is the angle between the vertical line and the line connecting the observation point to the object [22]. This angle is measured from 0° to 90° , where 0° corresponds to the vertically upward direction, and 90° corresponds to the direction lying in the horizontal plane. In raytracing, the zenith angle θ is the angle between the ray

direction vector and the vector pointing along the vertical axis.

In the RTER v.2.0 software, the zenith angle θ of tracing is determined through a point on the ellipsoidal reflector side surface, which is defined by the intersection with a plane perpendicular to the major ellipsoid axis and located at a certain distance $[-z; z]$ from the ellipsoid center O , where $z = a -$ the major ellipsoid semi-axis (Figure 5).

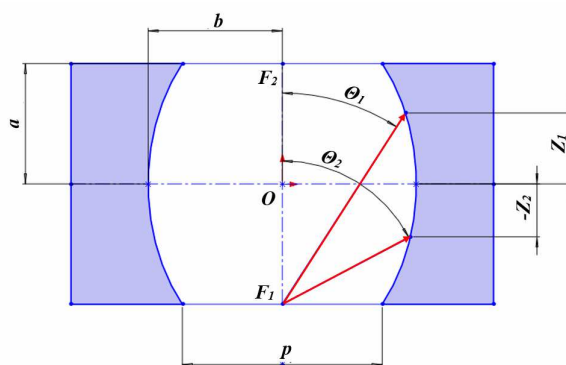


Fig. 5. Raytracing scheme in ellipsoidal reflector with different zenith angles θ_1 and θ_2

Figure 5 illustrates the raytracing in an ellipsoidal reflector with semi-axes a and b , focal parameter p , and focal points F_1 and F_2 , located in the first and second focal planes. The distance along the major ellipsoid axis from the center z_1 and the angle θ_2 by the distance z_2 determines the zenith angle θ_1 . To the side surface, a multivector tracing is performed in the ellipsoidal reflector with an eccentricity $e = 0.667$ and a focal parameter $p = 16.67$ mm within the azimuthal angle range $\varphi \in [0; 2\pi]$ with a step of $0,01$ rad $\cdot\pi$ and initial point steps of 0.34 mm, while varying the zenith angle $\theta \in [22.61^\circ; 90^\circ]$. Figure 6 shows the graphical result of the multivector tracing for zenith angles of 90° , 45.39° , and 30.17° .

To interpret the obtained results in graphs and evaluate them, the zenith angle limits θ were calculated for each run, starting from the center of the focal plane, i.e., from the focus F_1 , as well as at the edge of the focal circle. It is explained by the zenith angle θ variation at each step of the ray exit points along the radius vector during multivector tracing (Table 1).

The calculation results of the Centroid parameter were obtained to evaluate the tracing properties of the ER side surface. The Centroid represents the average coordinates value where the rays intersect the ER side surface from the focal plane with different zenith angles (Figure 7). These coordinates are used to measure the displacement of the image center relative to the focal plane center, which can be caused by the aberrations' presence [23].

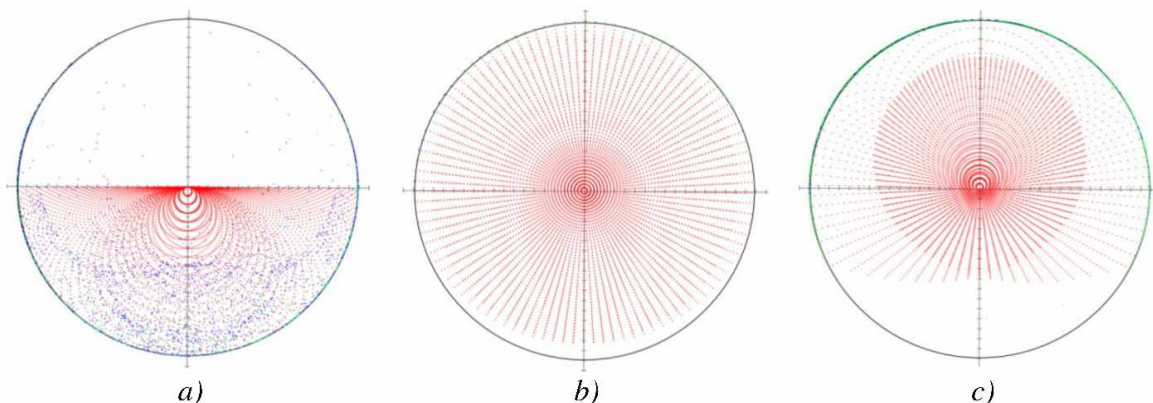


Fig. 6. Multivector tracing visualization along the radius for zenith angles: 90° (a), 45.39° (b), and 30.17° (c)

Table 1. Zenith angle θ limits depending on the ellipsoid center distance.

Distance from the center of the ellipsoid, mm	Distance from the first focal plane, mm	Zenith angle θ for rays exiting the focal circle, degrees	Zenith angle θ for rays exiting F1, degrees
-20.2577	0	90	90
-18.2319	2.02577	31.43	83.62
-16.2062	4.05154	29.35	78.05
-14.1804	6.07731	27.41	73.11
-12.1546	8.10308	25.57	68.67
-10.1289	10.12885	23.83	64.61
-8.10308	12.15463	22.15	60.88
-6.07731	14.18040	20.53	57.41
-4.05154	16.20617	18.96	54.16
-2.02577	18.23194	17.42	51.09
0	20.25771	15.9	48.18
2.025771	22.28348	14.39	45.39
4.051542	24.30925	12.9	42.71
6.077313	26.33502	11.4	40.11
8.103084	28.36079	9.9	37.57
10.12885	30.38656	8.38	35.09
12.15463	32.41234	6.83	32.63
14.1804	34.43811	5.23	30.17
16.20617	36.46388	3.58	27.71
18.23194	38.48965	1.85	25.2
20.25771	40.51542	0	22.61

Figure 7 shows a significant correlation between the results for the x and y coordinates. Therefore, in further research, it is sufficient to have data obtained for only one of the coordinates. The deviations of the Centroid are negligible for more than three reflection acts. The highest values are observed for tracing at azimuthal angles θ ranging from 22.6° to 30°, smoothly approaching zero at $\theta = 48.18^\circ$, corresponding to the azimuthal angle that intersects the minor ellipsoid axis passing through ER center. In the range of θ from 48.18° to 90°, the deviations increase and become negative. It is also worth noting that the deviations decrease by an

average of 60% with an increase in the reflection acts number in the range of θ from 30° to 90°.

RMS is a metric for measuring aberrations (deviations) of points in an optical system. The RMS coordinates of the ray intersection points in the second focal plane provide information about the distribution of aberrations and their overall level.

A lower RMS value indicates a minor impact of aberrations, indicating higher optical system quality. Figure 8 shows the dependence of RMS coordinates for different reflection acts as the zenith angle θ changes.

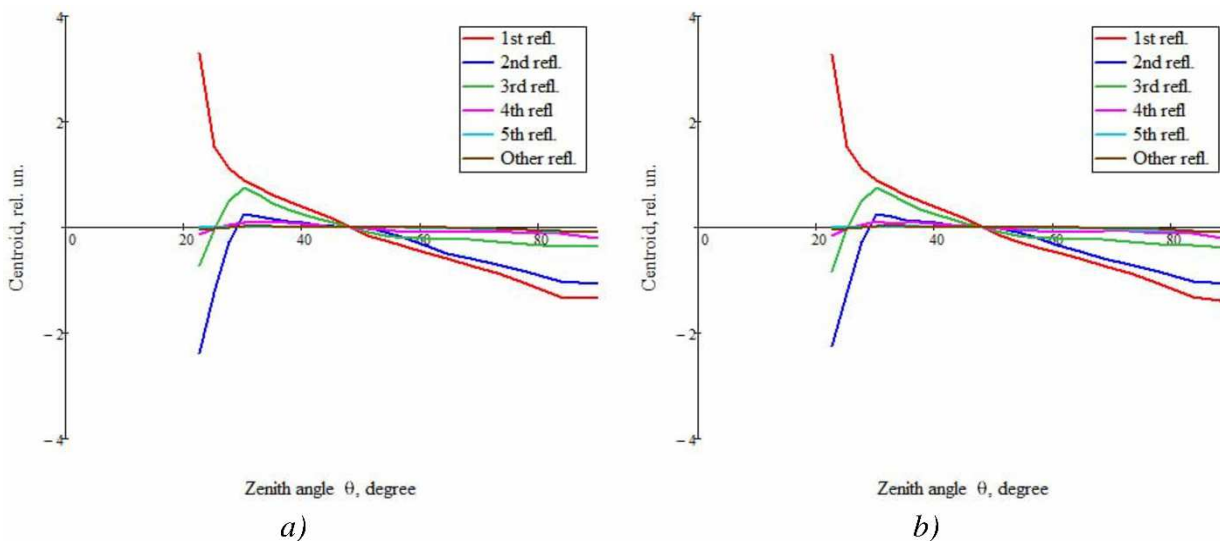


Fig. 7. Centroid coordinates x (a) and y (b) dependence on the zenith angle θ for raytracing (by radius) in the ellipsoidal reflector for different reflection acts numbers

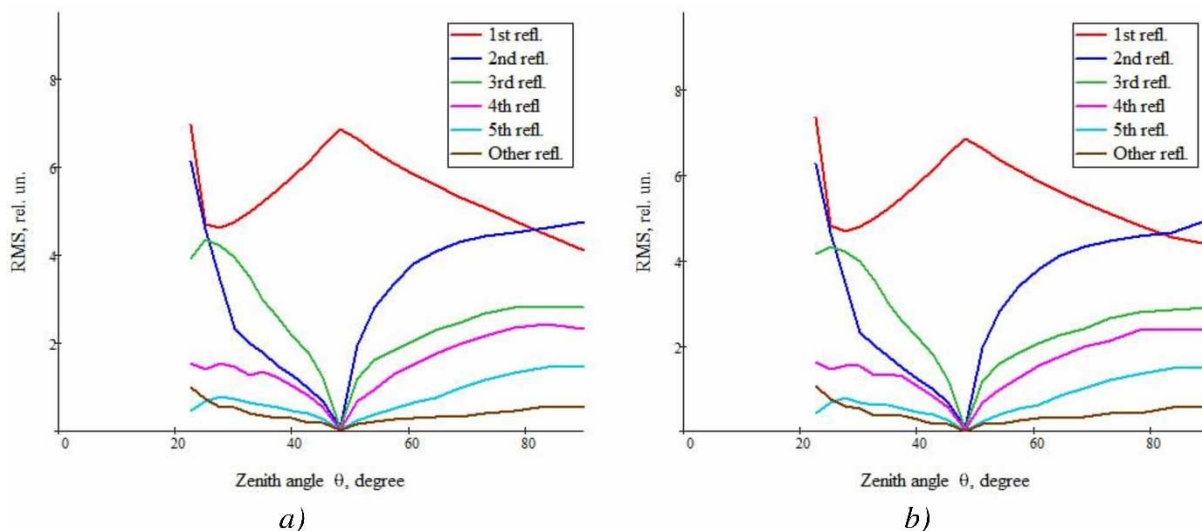


Fig. 8. RMS coordinate x (a) and y (b) dependence on the zenith angle θ during raytracing in ellipsoidal reflector for different reflection acts numbers

Conclusions

The paper presents an information system for multi-vector analysis in ellipsoidal reflectors results. An algorithm for multi-vector tracing has been developed, based on which the RTER v.2.0 software has been created. This software allows for selecting the tracing mode, configuring launch parameters, and setting the step of ray launch points. It provides the flexibility to use different methods of multi-vector tracing: by radius, by diameter, and by being radius part, thus enhancing the versatility of RTER v.2.0 for different types of tasks and expanding the capabilities for visualizing the obtained simulation results.

Based on the multi-vector aberration analysis of the ellipsoidal reflector side surface with an eccentricity of $e = 0.667$ and a focal parameter of $p = 16.67$ mm, it has been established that the deviations of the centroid coordinates are insignificant for

reflections beyond the third one, with the highest values observed at azimuthal angles θ from 22.6° to 30° . The root mean square deviations of the coordinates decrease by approximately 50% with an increase in the reflections count, except for the first reflection at a zenith angle of $\theta = 48.18^\circ$, which exhibits an inverse pattern.

The obtained dependencies of zenith angles on coordinate deviations can improve the ellipsoidal reflectors and optical systems of photometers designed for various purposes by developing additional tools to aberrations compensate for or modify the reflector side surface shape.

References

- [1] J. M. Sasian, *Introduction to Lens Design*. Cambridge University Press, 2019.

- [2] D. Aguirre-Aguirre, D. González-Utrera, B. Villalobos-Mendoza, and R. Díaz-Urbe, "Fabrication of biconvex spherical and aspherical lenses using 3D-printing", *Applied Optics*, vol. 62, no. 8, pp.C14-C20, 2023. DOI: 10.1364/AO.477347.
- [3] T. Laramy-K. *Principles of Atoric Lens Design*. Laramy-K Optical, 2010.
- [4] Shenzhen Sian Communications Technology Co, "Non-spherical lens design method and non-spherical lens", CN2008100668737A, Sep. 24, 2008.
- [5] K. O. Sugisaki, M. Tetsuya, and W. Katsuhiko, "Assembly and alignment of three-aspherical-mirror optics for extreme ultraviolet projection lithography", in *Proceedings of SPIE - The International Society for Optical Engineering*, 2000. DOI: 10.1117/12.390114.
- [6] U. Ceyhan, "Characterization of aspherical lenses by experimental ray tracing", thesis of Doctor of Philosophy in Electrical Engineering, Jacobs University, 2013.
- [7] Y. Chen, X. Wang, C.D. Zhou, and Q. Wu, "Evaluation of visual quality of spherical and aspherical intraocular lenses by Optical Quality Analysis System", *International Journal of Ophthalmology*, vol. 10, no. 6, pp.914-918, 2017. Doi: 10.18240/ijjo.2017.06.13.
- [8] M. Bezuglyi, I. Sinyavski, N. Bezuglaya, і A. Kozlovskiy, "Особливості виготовлення еліпсоїдальних рефлекторів фотометрів", *Bull. Kyiv Polytech. Inst. Ser. Instrum. Mak.*, вип. 52(2), с. 76–81, Груд 2016.
- [9] Н. Безугла, С. Полукетов, В. Чорний, і М. Безуглий, "Монте-Карло симуляція світлорозсіяння шарами шкіри людини методами просторової фотометрії", *Bull. Kyiv Polytech. Inst. Ser. Instrum. Mak.*, вип. 61(1), с. 91–100, Чер 2021. DOI:10.20535/1970.61(1).2021.237112
- [10] N. V. Bezuglaya, A. A. Haponiuk, D. V. Bondariev, S. A. Poluectov, V. A. Chorny, and M. A. Bezuglyi, "Rationale for the Choice of the Ellipsoidal Reflector Parameters for Biomedical Photometers", *Devices and Methods of Measurements*, vol. 12, no. 4, pp. 259-271, 2021. Doi: 10.21122/2220-9506-2021-12-4-259-271.
- [11] J. A. R. Samson, and D. L. Ederer, "Imaging Properties and Aberrations of Spherical Optics and Nonspherical Optics", *Experimental Methods in the Physical Sciences*, Academic Press, vol.31, pp. 145-181, 1998. DOI: 10.1016/S0076-695X(08)60043-5.
- [12] H. S. Kim, K. Y. Park, W. K. Lee, and J. U. Jeon, "Design of Spherical Aberration Free Aspherical Lens by Use of Ray Reverse Tracing Method", *Journal of the Korean Society for Precision Engineering*, vol. 20, no. 10, pp.191-198, 2003.
- [13] C. Henning, T. Fleischmann, and F. Hilbig, "Measurements of aberrations of aspherical lenses using experimental ray tracing", in *Proc SPIE*, 2011. DOI: 10.1117/12.895009.
- [14] S. Giovanzana, H. Kasprzak, and B. Pałucki, "Non-rotational aspherical models of the human optical system", *Journal of Modern Optics*, vol. 60, no. 21, pp. 1898-1904, 2013. DOI: 10.1080/09500340.2013.865802.
- [15] N. Hiroshi, Two-Dimensional Ray Tracing. *John Wiley & Sons, Singapore Pte. Ltd.*, 2015. doi: 10.1002/9781118939154.ch4.
- [16] G. H. Spencer, and M. V. R. K. Murty, "General Ray-Tracing Procedure", *Journal of Optical Society of America*, vol. 52, no. 6, pp. 672-678, 1962.
- [17] J. E. Gómez-Correa, J. Coello, V. Garza-Rivera, and A. Puente, "Three-dimensional ray tracing in spherical and elliptical generalized Luneburg lenses for application in the human eye lens", *Applied Optics*, vol.55, pp.2002-2010, 2016. DOI: 10.1364/AO.55.002002.
- [18] C. Y. Hu, and C. H. Lin, "Reverse Ray tracing for transformation optics". *Optics express*, vol.23, pp.17622-17637, 2015. DOI: 10.1364/OE.23.017622.
- [19] M. Epstein, D. Peter, and M.A. Slawinski. "Combining Ray-Tracing Techniques and Finite-Element Modelling in Deformable Media", *The Quarterly Journal of Mechanics and Applied Mathematics*, vol. 65, no. 1, pp.87-112, 2012. DOI: 10.1093/qjmam/hbr021.
- [20] M. A. Bezuglyi, N. V. Bezuglaya, and I. V. Helich, "Ray tracing in ellipsoidal reflectors for optical biometry of media", *Applied Optics*, vol. 56, no. 30, pp. 8520 – 8526, 2017. DOI: 10.1364/AO.56.008520
- [21] М. О. Безуглий, та Р. О. Молодик, "Комп'ютерна програма «Трасування променів в еліпсоїдальному рефлекторі»" (Ray Tracing in Ellipsoidal Reflector) ("RTER"), *Свідчення про реєстрацію авторського права на твір № 67015*, 04.08.2016
- [22] T. Sato, "Analytical Model for Estimating the Zenith Angle Dependence of Terrestrial Cosmic Ray Fluxes", *PLoS ONE*, vol. 11, no.8, 2016. doi: 10.1371/journal.pone.0160390.
- [23] C. Zhai, M. Shao, R. Goullioud, and B. Nemati, "Micro-pixel accuracy centroid displacement estimation and detector calibration", in *Proceedings of The Royal Society A Mathematical Physical and Engineering Sciences*, 2011. DOI: 10.1098/rspa.2011.0255.
- [24] A. Torben, "Evaluating rms spot radii by ray tracing", *Applied Optics*, vol. 21, pp. 1241-1248, 1982. DOI: 10.1364/AO.21.001241.
- [25] F. B. Abdalla, A. Marins, P. Motta, and E. Abdalla, "The BINGO Project - III. Optical design and optimization of the focal plane",

УДК 535.2:616-71

¹⁾Полуектов С. О., ¹⁾Безугла Н. В., ²⁾Куровська-Вільчинська К. та ¹⁾Безуглий М. О.¹⁾Національний технічний університет України «Київський політехнічний інститут імені Ігоря Сікорського», Київ, Україна²⁾SWPS Університет, Варшава, Польща**ІНФОРМАЦІЙНА СИСТЕМА БАГАТОВЕКТОРНОГО ТРАСУВАННЯ ПРОМЕНІВ В ЕЛІПСОЇДАЛЬНИХ РЕФЛЕКТОРАХ**

Еліпсоїдальні рефлектори завдяки наявності двох фокусів є унікальними дзеркальними оптичними елементами, що дозволяють спряжено формувати зображення в двох фокальних площинах в межах внутрішньої порожнини. Такі рефлектори використовуються в багатьох пристроях, наприклад в лінзових телескопах для забезпечення високої роздільної здатності. Вони знайшли своє застосування в оптичних системах мікроскопів для збільшення зони різкості, використовуються в оптичних приладах для наукових досліджень, наприклад, в лазерних системах для забезпечення високої точності та стабільності лазерного променя.

Несферична форма еліпсоїдальних рефлекторів, окрім своїх переваг, має й недоліки: виникнення похибок в результаті трасування променів бічною поверхнею, що ускладнює абераційний аналіз та потребує спеціалізованих програмних забезпечень для проведення багатовекторного трасування. Врахування відхилень координат точок перетину променями з другою фокальною площиною дозволить оптимізувати конструкцію рефлектора для досягнення найбільшої ефективності. Тому метою даної роботи є підвищення ефективності абераційного аналізу еліпсоїдальних рефлекторів внаслідок розробки принципів та інформаційних засобів багатовекторного трасування променів.

У роботі представлені результати розробки інформаційної системи для проведення багатовекторного аналізу в еліпсоїдальних рефлекторах. Розроблений алгоритм багатовекторного трасування дозволив здійснити вибір режимів трасування, налаштування параметрів запуску та встановлення кроку точок запуску променів. Представлено особливості спеціалізованого програмного забезпечення при одно- та багатовекторному трасуванні променів в еліпсоїдальному рефлекторі. Цільовим об'єктом дослідження є бічна поверхня еліпсоїда. У програмно забезпеченні реалізовано можливість використання різних способів багатовекторного трасування променів: за радіусом, за діаметром та за частиною радіусу для різних типів задач, що розширює можливості для візуалізації результатів моделювання.

На підставі багатовекторного абераційного аналізу функціонування бічної поверхні еліпсоїдального рефлектора отримано значення відхилень координат центру та середньоквадратичного відхилення координат для різних актів відбиття при зміні зенітного кута трасування. Оцінено вплив зенітних кутів на відхилення координат, що може бути використано при виборі параметрів еліпсоїдальних рефлекторів та конструкції оптичної системи фотометрів різного призначення, а також проектуванні додаткових засобів для компенсації аберацій або зміни форми бічної поверхні рефлектора.

Ключові слова: еліпсоїдальний рефлектор; трасування променів; багатовекторність; абераційний аналіз; Centroid; RMS.

Надійшла до редакції
23 квітня 2023 року

Рецензовано
18 травня 2023 року



© 2023 Copyright for this paper by its authors.
Use permitted under Creative Commons License Attribution 4.0 International (CC BY 4.0).